ADVANCED MATERIALS INTERFACES
www.advmatinterfaces.de

Nanoscale Adhesive Properties of Graphene: The Effect of Sliding History

*Xin-Z. Liu, Qunyang Li, Philip Egberts, and Robert W. Carpick**

Single-asperity adhesion between nanoscale silicon tips and few-layer graphene (FLG) sheets, as well as graphite, was measured using atomic force microscopy (AFM). The adhesion mechanism was understood through experiments and finite element method (FEM) simulations by comparing conventional pull-forces measurements (contact and separation, without sliding) to those obtained after the tip was slid along the surface before separation ("pre-sliding"). Without pre-sliding, no variation in the pull-off force was measured between consecutive measurements, and there was no observable dependence of the mean pull-off force value on the number of FLG layers. However, when the tip was pre-slid over a local area, the first pull-off force was enhanced by 12–17%; subsequent pull-off forces then relaxed to a lower, constant value. This occurred regardless of the number of layers, and occurred for aged graphite samples as well. Our analysis indicates that this is due to sliding-induced changes of graphene's interfacial geometry, whereby local delamination of the top graphene layer occurs, provided there is sufficient atmospheric exposure of the surface after cleaving. This effect provides another unique feature of the nanotribological behavior of atomically-thin sheets and is consequential for designing graphene-based devices and coatings where adhesive interactions are important.

1. Introduction

Since its production as isolated few-layer sheets in 2004,[1] graphene has attracted tremendous attention because of its many superior and remarkable properties (*e.g.*, electronic, thermal, mechanical, and tribological properties). Potential applications of graphene include transparent electrodes,[2] ultrahigh frequency transistors,[3] impermeable chemical barrier,[4–7] and micro- and nanoelectromechanical systems (MEMS/NEMS).[8] To date, a large number of studies have been devoted to the electronic,[9,10] and thermal properties[11] of graphene.

There are fewer studies of the mechanical and tribological properties of graphene, but these studies demonstrate that graphene exhibits remarkable mechanical and tribological properties as well. For example, macroscale frictional properties of graphene prepared by various methods (*e.g.* chemical vapor deposition-grown (CVD), exfoliated, and epitaxial graphene) showed a friction coefficient lower than bulk graphite,[12,13] suggesting a possible application as a solid lubricant. At the nanoscale, Lee *et al.* reported exfoliated graphene as the strongest material ever measured,[14] and the strength of CVD graphene is only slightly lower than that of exfoliated graphene.[15] Filleter *et al.* showed that a single layer of epitaxial graphene has higher friction than a bilayer.[16] This phenomenon was later also observed on other exfoliated two-dimensional (2-D) materials by Lee *et al.*[17] The monotonic decrease in friction from single to multiple layers was proposed to be a universal property of 2-D materials if the material is not strongly adhered to a supporting substrate.[17] This layer-dependent "strengthening" (an increase in friction force along the sliding direction, until a saturation level was reached) is proposed to be a result of a thin-film puckering effect: thinner atomic sheets are more susceptible to out-of-plane deformation than thicker sheets, resulting in out-of-plane deformation of all layers of the graphene around the tip due to tip-graphene adhesion, leading to larger contact areas and thus higher friction forces.[17] For graphite, Deng *et al.*[18] recently reported that exposing the surface to ambient air increases the interaction between the AFM tip and top graphite layer; correspondingly, the top-layer adheres strongly to the tip and locally delaminates when the tip slides over it at a tensile load, leading to a marked increase in friction as the load is decreased. This study focused on frictional effects as opposed to the dependence of adhesion on sliding.

Despite these advances in understanding the trends observed for the friction response of graphene, results from recent studies on adhesion between graphene sheets and an interacting counter-surface[19–22] have not produced clear

X.-Z. Liu, Prof. Q. Li,[+] Prof. P. Egberts,[++]
Prof. R. W. Carpick
Department of Mechanical Engineering
and Applied Mechanics
University of Pennsylvania
220 S. 33rd Street, Philadelphia, Pennsylvania, 19104, USA
E-mail: carpick@seas.upenn.edu
Prof. Q. Li
Department of Engineering Mechanics
Tsinghua University
Beijing, 100084, China
[+]Present address: Department of Engineering Mechanics, Tsinghua University, Beijing 100084, China
[++]Present address: Department of Mechanical and Manufacturing Engineering, Schulich School of Engineering, University of Calgary, Calgary, Alberta, Canada, T2N 1N4

DOI: 10.1002/admi.201300053

trends (*e.g.,* as a function of the number of FLG layers) and specific mechanisms governing adhesion have not yet been described. Given that adhesion is important for many potential applications of graphene (*e.g.,* as a protective coating, in thin-layer devices, or for reducing surface friction), a better understanding of the adhesion behavior of graphene is desirable. In devices that use graphene as an integrated part of the structure, one must consider three different interactions: interfacial adhesion between the graphene and its substrate; adhesion between a moving asperity (*e.g.* an AFM tip, or an asperity on a counter-surface) and the graphene/substrate system; and for multilayer graphene films, the interaction between the graphene layers. To date, only a few studies have been devoted to explore these interactions with even fewer focused on the layer-dependence of adhesion.[20–23]

Both theoretical and experimental studies conducted to estimate the adhesive interaction between graphene and SiO_2 give a range of values for adhesion energies for graphene-SiO_2 interfaces.[19–23] These discrepancies may be due to substrate roughness,[24] substrate treatment, substrate morphology[23] *etc.*, and sliding history, as will be discussed in the paper.

In this paper, adhesive interaction between few-layer graphene (FLG) sheets on supporting substrates and single-asperity silicon tips (with a native oxide) is studied. Atomic force microscopy (AFM) is used to discern the number of FLG layers and to perform *in situ*, localized friction and adhesion measurements.[25] The pull-off forces between FLG samples and silicon tips are significantly affected by sliding the tip along the surface of graphene before conducting pull-off force measurements. We call this the "sliding history effect" in the subsequent sections. This proposed mechanism for the sliding history effect arises from local, transient top-layer delamination induced by sliding, leading to an enhancement of the pull-off forces. The effect requires strong intrinsic adhesion between the tip and the top-layer of the sample which is facilitated by extended exposure to a dry nitrogen purged atmosphere which will contain trace amounts of water and oxygen,[18,26] thus leading to oxidation. This is consistent with the mechanisms for the friction behavior proposed by Deng *et al.*[18] as discussed above.

2. Results

2.1. Direct Pull-Off Measurement

Figure 1(a) shows five datasets of 100 pull-off force values *vs.* the measurement number on FLG, measured by direct pull-off measurements, or force *vs.* distance (FD) measurements. The FLG regions had thicknesses ranging from 1 to 5 layers, with one dataset acquired for each number of layers. Within each

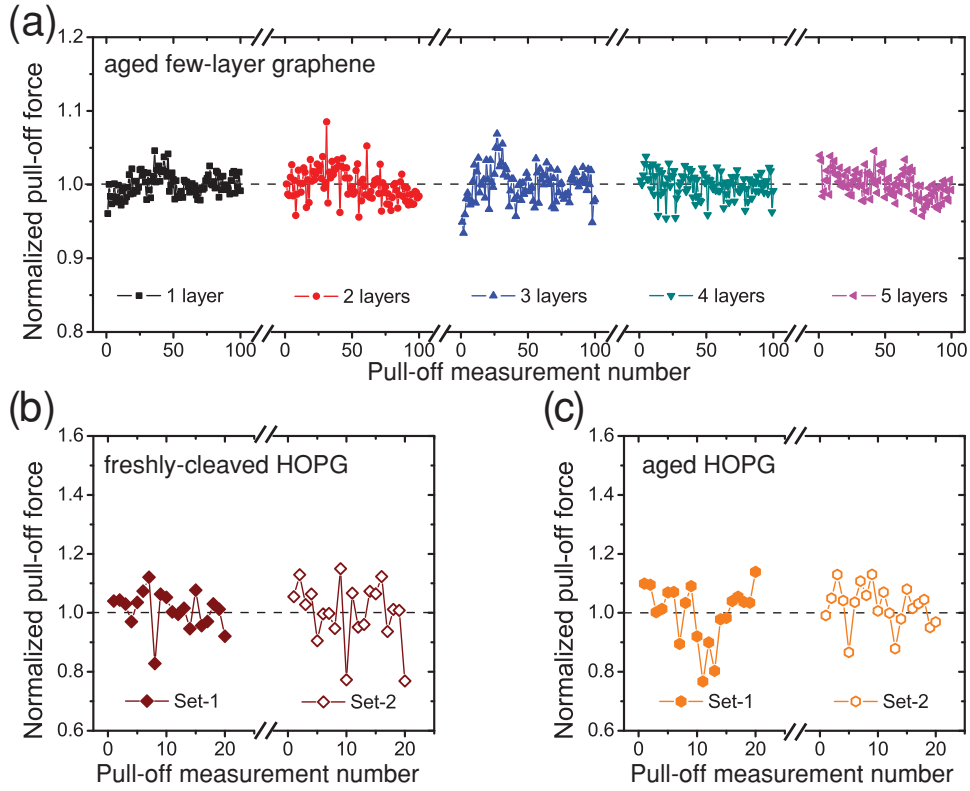

Figure 1. (a) Normalized pull-off forces versus measurement number on FLG with 1 to 5 layers, acquired using direct pull-off measurements. The measured pull-off forces have been normalized to their mean values in each set of connected data points. For reference, the mean pull-off force measured on the single layer graphene sample is 18.7 ± 0.4 nN; this is representative of the values measured throughout the experiments. Normalized pull-off forces versus pull-off measurement number for (b) freshly-cleaved and (c) aged graphite, respectively. In (b) and (c) the same tip was used. However, each "set" refers to pull-off forces measured in different regions of interest on the same sample. A gray dashed line indicates the mean value in each case.

dataset, pull-off forces are plotted in chronological order. In these measurements, pull-off measurement number 1 refers to the first measured pull-off force, 2 the second measured pull-off force, *etc*. The pull-off forces were normalized to the mean value measured for each set of measurements to better show the relative changes in the force. Figure 1(a) shows that the variation in pull-off forces measured at one area of interest does not vary significantly with increasing pull-off measurement number.

The absolute mean pull-off force measured on a single layer graphene in Figure 1(a) is 18.7 ± 0.4 nN. This magnitude is representative of the values measured throughout the experiments. Similar values were obtained on regions with more layers (see Supporting Information).We can estimate the corresponding work of adhesion by applying continuum adhesive contact mechanics,[27] and using an estimated tip radius of 15 ± 5 nm. This value is based both on manufacturer's values and on transmission electron microscopy measurements of tip radii we acquired for other tips of the same make and model as that used here. This value is thus representative of unused AFM tips. According to the Johnson-Kendall-Roberts (JKR) model,[28] this pull-off force corresponds to a work of adhesion of 0.26 ± 0.09 J/m^2 between the silicon tips and graphene. Similarly, when the Derjaguin-Müller-Toporov (DMT) model[29] is used, this pull-off force corresponds to a work of adhesion of or 0.20 ± 0.07 J/m^2. Averaging these two results in an overall mean estimated value of 0.23 ± 0.11 J/m^2.

In addition, direct pull-off force measurements were performed on freshly-cleaved graphite and aged graphite. In this case, each dataset consisted of 20 pull-off measurements within a given area of the sample, and two different areas of each sample were tested with the same tip. The results are plotted in Figures 1(b) and (c), which show that for both freshly-cleaved and aged graphite, respectively, the pull-off forces did not vary over the course of a direct pull-off measurement series, just as observed in Figure 1(a) for FLG. Furthermore, there was no significant change in the pull-off force trends measured on different regions of the freshly-cleaved and aged graphite samples.

Figure 2 shows the mean pull-off force as a function of the number of graphene layers for FLG as well as for freshly-cleaved bulk graphite. Approximately 100 measurements are taken for each thickness value. For a given test, the same tip was used to measure all pull-off forces on FLG flakes of different thicknesses and on graphite. In each test, the pull-off force values were normalized to the mean value obtained for the lowest number of graphene layers, to emphasize the variation in adhesion as a function of the number of layers. This normalization also allows a comparison between pull-off forces measured with the three tips by reducing the effect of variability in tip size and tip chemistry. Figure 2 shows that within the standard deviation of the measurement, there is no variation in the measured pull-off force as a function of the number of graphene layers. Figure 2 shows that the pull-off forces measured on graphite (100's layers) were slightly lower on average than for FLG. However, the difference is within experimental uncertainty for Tips 1 and 2, and we note that the graphite sample had less air exposure than the FLG samples prior to insertion into the AFM chamber. The reduced air exposure of freshly cleaved graphite compared to FLG samples is due to the different amounts of time required for sample preparation in each case: the graphite can be cleaved, inserted in the AFM, and measured within as little as 10 minutes; FLG, on the other hand, requires optical microscopy and Raman imaging to identify the number of layers of graphene that are then targeted for subsequent AFM measurements.

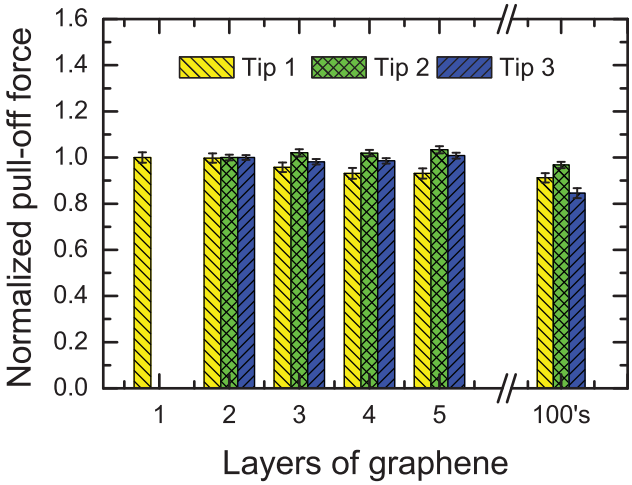

Figure 2. Normalized pull-off forces versus number of layers of graphene. The same tip was used within one test, and a single area investigated for each bar plotted. The number of layers was varied with a random order. Different tips and FLG samples were used in the three tests. Each test on graphite (100's layers) was performed on an N_2-aged sample, using the same tip used for the other FLG samples indicated for that test. Error bars represent the standard deviation in the mean value of the normalized pull-off force for each FLG or graphite sample (approximately 100 measurements acquired for each).

2.2. Pre-Sliding Pull-Off Measurement

In direct pull-off force measurements, lateral sliding of the tip does not occur, beyond the small amount of in-plane displacement that occurs (approximately 10% of the vertical extension, or ~10 nm) during a FD spectroscopy resulting from the 22.5° tilt angle between the cantilever and the surface normal,[28] which is intrinsic to the experimental protocol. Pull-off measurements were repeated using a "tilt compensation" protocol[30] that greatly reduces this in-plane displacement, and the trends were the same. The previously-reported dependence of friction on the number of layers involves prolonged lateral sliding (several μm) of the tip with respect to the sample.[17] These prior friction results suggest that it is insufficient to measure adhesion using only the direct pull-off technique, as it does not include the influence of sliding history on the interface. Using the pre-sliding test protocol, the pull-off force acquired includes the effect of prior tip sliding on the pull-off force on the first instant the contact between the sample and tip is broken.

Figure 3 shows the consecutive pull-off forces acquired after pre-sliding the tip on FLG samples, a freshly-cleaved graphite sample, and an aged graphite sample. In the same manner as Figure 1(a), Figure 3(a) shows the pull-off force recorded with increasing pull-off measurement number for FLG samples

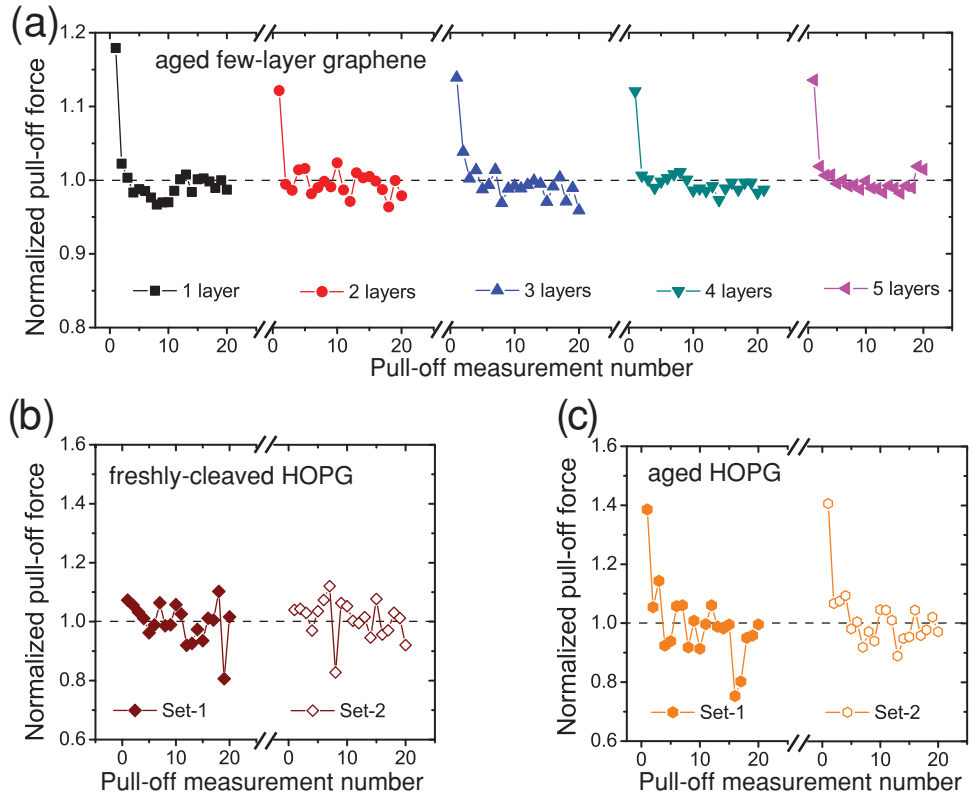

Figure 3. (a) Normalized pull-off forces versus measurement number on FLG with 1 to 5 layers, acquired using the pre-sliding methodology. The pull-off forces of the each set (connected with a solid line) have been normalized to the mean values of that particular set (represented by a grey dashed line). The measurements on graphene come from a single sample and have all been conducted using the same tip. The same pre-sliding measurement carried out on (b) freshly-cleaved graphite and (c) aged graphite. In (b) and (c) the same tip has been used in both "sets", but measurements have been performed on different regions of interest that are far away from each other. The pull-off forces have been normalized to the mean value of the dataset (grey dashed line).

of different numbers of layers (1–5). In Figure 3(a), the value marked by the gray dashed line represents the steady-state response used for normalizing the data and is based on the mean value of the 20 data points for each sample. This removes the effect of the transiently high values observed during the first few pull-off force measurements. The same measurements were also performed on freshly-cleaved graphite, Figure 3(b), and aged graphite, Figure 3(c), respectively. The first pull-off force measured is significantly higher than the pull-off forces subsequently measured for graphene (Figure 3(a)) and for aged graphite (Figure 3(c)) surfaces. Specifically, the pull-off force measured for FLG were 12–17% higher for pull-off measurement number 1 in comparison to subsequently measured pull-off forces. However, freshly-cleaved graphite (Figure 3(b)) shows no transient change in the measured pull-off force.

Figure 4 shows the mean value of the first pull-off force measured (normalized to the mean value of the 20 pull-off forces that are equivalent to the steady-state values found, indicated by the dashed line) for all layers of FLG and aged graphite. The data presented involves the normalized values acquired using multiple tips and different samples, totaling over 1000 pull-off measurements. For example, in the case of FLG, the data acquired is from more than 100 different pull-off force measurements for each layer number. As in the case

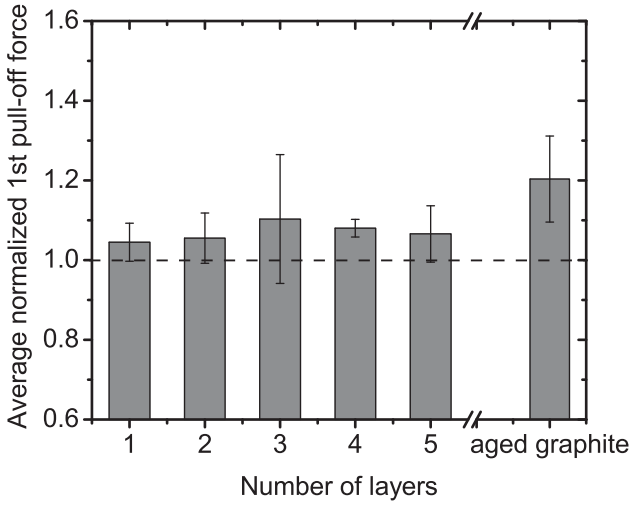

Figure 4. Mean pull-off forces of the first data point of all datasets of pull-off force measurements collected, normalized beforehand in a manner described earlier. The mean values for each FLG layer number and for aged graphite was calculated from over 100 measurements of an increased pull-off force during pre-sliding measurements. Error bars represent the standard deviation obtained from averaging the first data points for each layer number.

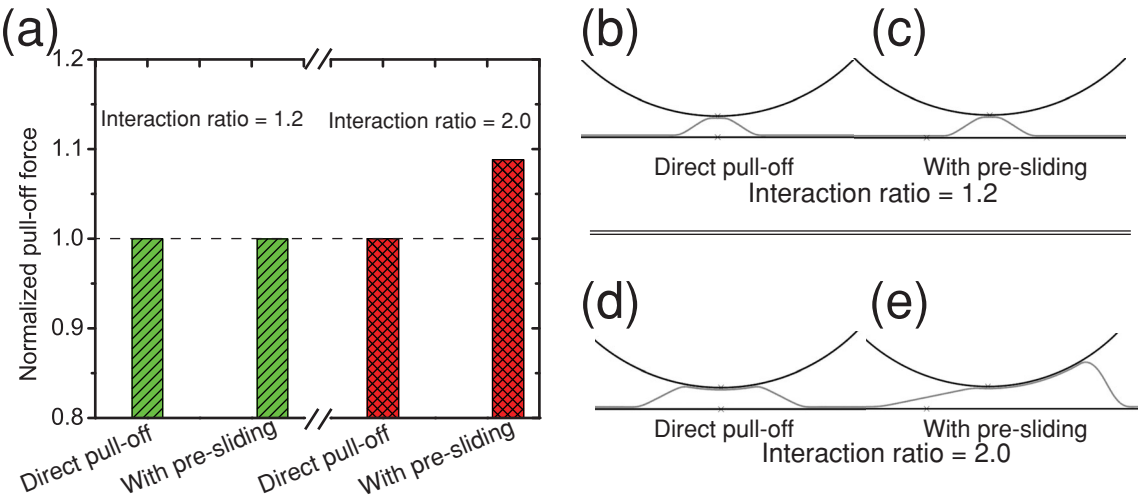

Figure 5. (a) FEM simulation results for normalized pull-off forces for interaction rations of $w_{tip-gr}/w_{gr-sub} = 1.2$ (green) and 2.0 (red) using direct pull-off measurements and with pre-sliding. The direct pull-off force is the same as that with pre-sliding for an interaction ratio of 1.2, whereas an interaction ratio of 2.0 results in an increase of ~9% compared to direct pull-off. (b) and (c) show excerpts from simulations with interaction ratio 1.2 for direct pull-off and with pre-sliding, respectively. The same for (d) and (e) is shown but with interaction ratio 2.0.

of the direct pull-off measurements, the error bars represent the standard deviation in the calculated mean value. Figure 4 shows that the first pull-off force is significantly higher than subsequent values. Furthermore, there is no statistically significant variation in the measured value of first pull-off force for graphene with the number of graphene layers.

2.3. FEM Simulations

FEM simulations of single-layer graphene were conducted to gain mechanistic insight into observed behavior. The two different types of AFM pull-off experiments were simulated: direct pull-off, and pre-sliding pull-off. We also investigated the effect of changing the adhesive interaction between the tip and the graphene relative to the graphene-substrate interaction. In the FEM simulations, only the first pull-off force is measured, as opposed to the AFM measurements where many subsequent pull-off forces are measured. The results of these simulations are shown in **Figure 5**. Figure 5(a) shows that there is no difference in the pull-off force measured in both direct pull-off and with pre-sliding when the ratio between the tip-graphene interaction strength, w_{tip-gr}, and the graphene-substrate interaction strength, w_{gr-sub}, is 1.2, representing the case where the sample is not aged. Figures 5(b) and (c) show snapshots of the FEM simulation during a pull-off measurement via the direct pull-off and the pre-sliding pull-off methods, respectively. The deformation of the graphene film is the same during pull-off measurements in direct pull-off and pre-sliding pull-off measurements. However, when the ratio w_{tip-gr}/w_{gr-sub} is increased to 2.0 to represent the case of an aged sample where the topmost layer has higher adhesion, there is a ~9% higher measured pull-off force in pre-sliding experiments compared to direct pull-off experiments. Figure 5(d) and (e) show snap-shots of tip, graphene film, and substrate during the pull-off simulation. Figure 5(d) shows that in direct pull-off force measurements, the graphene film is symmetric around the tip and lifting off the substrate. However, Figure 5(e) shows that pre-sliding drastically changed the interface configuration: at the same tip-substrate separation distance, the graphene film exhibits a greater amount of delamination for the case of pre-sliding than direct pull-off, as well as a greater contact area at the point of snap-out, yielding a greater pull-off force.

3. Discussion

In direct pull-off measurements (Figure 1), the pull-off forces did not change over a set of 100 measurements. The mean pull-off force observed on a single layer of graphene is 18.7 ± 0.4 nN, corresponding to an average value of 0.23 ± 0.11 J/m^2. This average value is well in the range of other values reported in the literature.[20–22] Only a slight variation in the direct pull-off force data is observed, suggesting that the contact geometry of the tip and graphene does not evolve significantly over the course of measurement. These slight variations are likely due to changes in local morphology or roughness of the substrate, as previously reported in the literature.[22–24] Similar results were also obtained on both freshly-cleaved and aged graphite, although the standard deviations are higher than that observed for FLG. The origin of this variation is not understood. Figure 2 shows a weak but statistically insignificant variation in measured direct pull-off forces on FLG as pull-off measurements are repeated, which is consistent with previously reported adhesion measurements in the literature.[17,22] Further experiments conducted on different number of layers of FLG in laboratory air (see Supporting Information) also show a negligible variation in the measured pull-off forces with the number of layers.

These observations of direct pull-off forces with insensitivity to the number of graphene layers are in apparent contrast to the previously-reported layer-dependent friction force on graphene. A reduction in friction force of approximately ~50% is observed for four layer FLG in comparison to one layer.[17] The mechanism behind the layer-dependent friction is explained by the

lower bending stiffness of single layer graphene. Being more susceptible to out-of-plane elastic deformation, higher friction occurs than for thicker sheets because adhesion and friction forces lead to larger contact areas between the tip and graphene. However, in direct pull-off force measurement (without pre-sliding of the tip), no variation was observed in the work of adhesion as a function of number of layers. Thus, the total intrinsic adhesive interaction, which is due primarily to van der Waals forces, does not depend observably on the number of layers. Thus, as postulated previously, the observed dependence of friction on the number of layers is not due to changes in tip-sample adhesion. Furthermore, it suggests that the contact geometry in direct pull-off force measurements is rather different than what is produced during friction measurements. A possible explanation for the layer-insensitive pull-off force measurements may be that adhesion forces are dominated by surface interactions between the AFM tip and the graphene surface. FEM results in Figure 5(b) and Figure 5(d) show that the graphene sheet deforms symmetrically under tensile forces, consistent with literature.[31] This symmetric deformation of the graphene sheet during pull-off measurements is likely to be isolated to the topmost graphene layer in either the FLG or bulk graphite samples, resulting in a layer-independent pull-off force. A FEM simulation with different numbers of layers will be discussed in detail elsewhere.

The steady-state pull-off forces observed in pre-sliding pull-off measurements on FLG in Figure 3(a), *i.e.*, the pull-off forces recorded at pull-off measurement numbers greater than 5 (or often less), show similar trends as those determined from direct pull-off measurements (Figure 1(a)). Similar trends are also observed for measurements performed on freshly-cleaved and aged graphite for the steady state values measured in pre-sliding measurements in Figure 3(b) and (c) respectively, as well as for those measured on the same sample using the direct pull-off measurement technique as shown in Figure 1(b) and (c), respectively. This result indicates that after at most 5 pull-off measurements, the contact between the AFM tip and the sample is not affected by previous sliding. However, the increase in the first pull-off force measurement shown in Figure 3(a), which can be up to ~17% higher than the steady state value, demonstrates that the nature of the interface just before the first pull-off measurement after sliding must be distinct from the other situations.

The variation in the initial enhancement of the pull-off force in pre-sliding measurements (Figure 4) is independent on the number of layers. Hence, the thin-film puckering effect that has strong influences on friction measurements cannot solely be responsible for the pull-off force enhancement since that effect depends on the number of layers, and furthermore, is absent for graphite. Using AFM, Deng *et al.* reported aging of graphite samples after cleavage when exposed to air increases the interaction between a sliding tip and the topmost graphite layer relative to the interlayer bonding between the bulk graphite layers.[18] We hypothesize that this mechanism is primarily responsible for the adhesion trends we observe in pre-sliding measurements.

This hypothesis is supported by two observations. First, as discussed above, the transient increase in pull-off force with pre-sliding, the steady-state pull-off force with pre-sliding, and the pull-off force from direct pull-off measurements are all independent of the number of layers, which includes the fact that a transient increase in the pull-off force also occurs on aged graphite. Thus, the phenomenon appears to be related to the state of the topmost graphene layer of the sample. Second, for freshly-cleaved graphite samples, no increase in pull-off force was observed in pre-sliding measurements, just as Deng *et al.* saw no increased tip-sample interaction for freshly-cleaved graphite.[18] These observations are consistent with the mechanism demonstrated by varying the adhesive interaction between the tip and substrate shown in the FEM simulation in Figure 5: aging the sample increases the adhesion between the topmost layer of graphene, and the structure of the graphene region around the contact is more strongly affected by sliding. We have further shown that if we impose a strong adhesive interaction between the graphene and the substrate, for example by examining one to three layers of graphene exfoliated onto freshly-cleaved muscovite mica, the transient increase in adhesion is again lost (see Supporting Information).

The proposed mechanism by which pull-off forces are enhanced after pre-sliding on graphene is illustrated schematically in **Figure 6**. Due to a low substrate-graphene interaction energy, the graphene loosely adheres to the substrate. Exposing the graphene to air (during sample preparation and the steps required to identify graphene on the substrate) results in aging of the top graphene layer (indicated by the red color), leading to an enhanced tip-graphene interaction that exceeds that of the graphene-graphene interlayer interaction. When the tip comes into contact, a symmetric pucker will form around the AFM tip as shown in Figure 6(a). Upon sliding in Figure 6(b), the symmetric pucker on the top-layer transforms asymmetrically

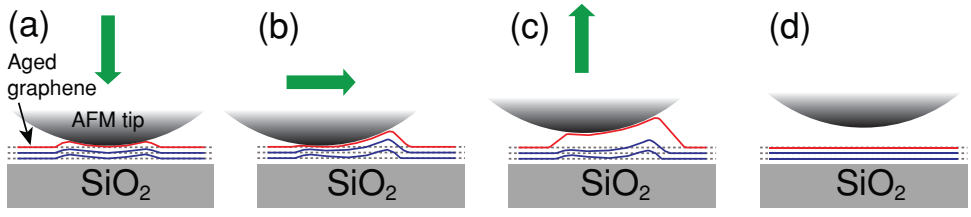

Figure 6. A schematic view of the pre-sliding pull-off measurement. The bold, green arrows indicate the direction of the tip motion. The red line represents the top graphene layer that is aged and thus can delaminate due to its enhanced interaction with the tip. (a) The AFM tip makes initial contact with the graphene sheet prior to reciprocating over that local area. (b) While scanning in a reciprocating motion, a small, asymmetric pucker gradually develops due to adhesion and friction between the sample and the tip. (c) At the end of the sliding cycles, the tip retracts. Due to the strengthened tip-graphene interaction, the interfacial configuration has changed such that the top-layer locally delaminates. This enhances the pull-off force. (d) After retraction, the graphene sheet relaxes and returns to the undeformed state.

such that the pucker at the front edge of the tip is larger in comparison to the rear edge. The size of the pucker at the front is expected to depend on the thickness of the graphene, as inferred from the friction measurements in Ref. [17]. After some sliding distance, the pucker reaches a maximum, steady-state size, resulting in a maximum steady-state contact area. Tip sliding is then halted and the tip-graphene contact is assumed to not relax; the tip then begins to retract from the sample. This initial stage of a pre-sliding pull-off measurement is shown in Figure 6(c). Owing to the increased tip-graphene interaction, the interfacial configuration of the tip and top graphene layer changes significantly, leading the top layer to delaminate. The force required for separation is thus enhanced. This is consistent with the friction measurements of Deng *et al.*, who see enhanced friction when retracting after pre-sliding on aged graphite or graphene.[18]

Comparing the case of a few graphene layers or many layers (graphite) to a single layer of graphene, based on previously-reported friction measurements,[17] the single layer has a bigger pucker owing to its lower bending stiffness (associated with its low thickness). However, we observe that this does not lead to an even greater enhancement in the pull-off force compared to multiple layers. There are two competing factors which can contribute to this lack of layer dependence: (1) for multilayer samples, the interlayer interaction between the top graphene layer and second layer below is stronger than the interaction between monolayer graphene and the silicon oxide substrate. Therefore, there will be an additional force resisting the delamination of the top layer, which tends to increase the pull-off force for multilayers; and (2) there is an increased strain energy release rate for thinner layers due to the more highly deformed graphene around it. This will tend to decrease the pull-off force for thinner layers. These two competing effects, if similar in magnitude, can explain why the first pre-sliding-enhanced pull-off force for monolayer graphene (when weakly adhered to its substrate) is not significantly different than that for multilayers or for graphite. Full verification of these hypotheses would require detailed atomistic calculations which are beyond the scope of this paper. Finally, once the contact is broken, the top-layer pucker relaxes as shown in Figure 6(d), and subsequent measurements show lower pull-off forces in comparison to the first measured pull-off force. The steady-state value obtained during subsequent measurements is similar to the case obtained during direct pull-off measurement.

We note that in some of the sets of measurements, particularly Figure 3(a) for 1, 3, and 5 layers, and Figure 3(c) for both measurement sets of aged graphite, the relaxation to the steady-state value of the pull-off force is not immediate: the next two or three pull-off force measurements show a slightly enhanced pull-off force. This suggests that, in some cases, the relaxation of the region of graphene deformed by the pre-sliding persists over a surprisingly long time scale, as the time elapsed between successive pull-off measurements in Figure 3 is 1 s. The lack of consistency in observing this effect could be due to thermal drift, or due to inhomogeneities in the graphene surface chemistry. Further work is required to fully understand this effect.

To summarize, from this study we have a better understanding of the roles of the three adhesive interactions that altogether govern the response of the entire mechanical system: the interfacial adhesion between the graphene and its SiO_2 substrate; adhesion between a moving asperity and the graphene/substrate system; and the interlayer interaction for multilayer graphene films. Adhesive interactions between tip and graphene increase upon exposing the graphene surface to oxygen-containing environments. The effect of sliding history on the surface of FLG and graphite becomes important when the adhesive interaction between the surface and the tip exceeds the graphene interlayer bonding or the graphene/substrate adhesion. Finally, given the insensitivity of the pull-off force to the number of layers of FLG, the graphene-substrate adhesion and the graphene interlayer bonding is apparently relatively unaffected by chemical modification, in contrast to the tip-graphene interaction. This result is consistent with the previous literature demonstrating the chemical impermeability of graphene sheets.[21] Based on our picture of the adhesion behavior of graphene, we hypothesize that the effect of sliding history is localized to the topmost layer and does not influence subsequent layers in multilayer FLG. However, more work is needed to further investigate the nature of the graphene deformation below the top layer.

4. Conclusion

We performed experiments to investigate the nanoscale adhesion properties of graphene supported on silicon oxide using silicon AFM probes in nitrogen-purged environments. Although previous observations show that friction on graphene, as with other atomically-thin films, exhibits a strong dependence on the number of layers, direct pull-off measurements (with no pre-sliding) show that the pull-off force is independent of the number of graphene layers. Based on estimates of the tip radii used, the average work of adhesion between the silicon tips (which have a native oxide) and graphene is found, using continuum adhesive contact mechanics, to be 0.23 ± 0.11 J/m^2. However, if either graphene or graphite have been aged via exposure to air, or a N_2 atmosphere (which contains trace amounts of water and oxygen), and if the tip is pre-slid against the sample, the pull-off force is enhanced by 12–17% the first time the tip-sample contact is broken. The enhancement disappears after subsequent pull-off force measurements at the same location. The enhancement is not observed for thin graphene layers that were deposited on freshly-cleaved muscovite mica and then aged; nor was it observed on freshly-cleaved graphite.

These results indicate that aging of graphite and graphene films result in strengthening of adhesive interaction between a silicon tip and the topmost layer of graphene on the sample. This effect is seen to occur in FEM simulations of monolayer graphene using physically reasonable parameters. Based on results of Deng *et al.*[18], the aging process leads to some degree of oxidation of the surface, and this more polar surface interacts more strongly with the native oxide of the silicon AFM tip. When the interaction between the tip and the topmost layer of graphene/graphite is further enhanced by sliding, the tip-graphene interfacial configuration is substantially altered such that topmost layer locally delaminates under tensile loading, leading to an enhanced pull-off force. Upon subsequent pull-off force

measurements, the topmost graphene/graphite layer relaxes to the geometrical state it had before sliding. The effect is suppressed in FLG (1-3 layers) exfoliated onto freshly-cleaved muscovite mica because the strong interaction energy between the mica and the graphene prevents the local delamination. These measurements, or the observation of a sliding-dependent pull-off force, demonstrate the importance of the three interfaces (tip/graphene; graphene/graphene; and graphene/substrate) when measuring adhesion forces on 2-dimensional materials. It also shows that minimization of adhesion forces on graphene-terminated surfaces that will be exposed to oxygen-containing atmospheres can be attained by using 1 to 3 layers that are strongly adhered to the substrate.

5. Experimental Section

AFM Experiments: All experiments were conducted in a RHK UHV-350 AFM, where the chamber was purged by clean dry nitrogen obtained from the vapor of a liquid nitrogen dewar (relative humidity <2%, measurement limited by the hygrometer's range). The dry nitrogen environment (1 atmospheric pressure) reduces the possible effects of water adsorption and prevents meniscus formation at the contact. Silicon contact-mode AFM cantilevers (CSC 37, Mikromash Inc., specified tip radius R = 10–15 nm) were used as force sensors without further treatment, for all the experiments. These tips are terminated with a native silicon oxide layer having a thickness between 1–2 nm. The normal bending spring constant was calibrated using the Sader method,[32] resulting in force constants ranging from 0.05–0.4 N/m. The sensitivity of the photodetector was the determined by measuring the slope of cantilever deflection versus z-sample displacement signal in a pull-off measurement against a silicon substrate. Pull-off force measurements were conducted by performing pull-off measurements on several different samples, including mechanically-exfoliated graphene on SiO_2 wafers, freshly-cleaved graphite, and air-aged graphite.

Few-layer graphene (FLG) samples were produced by the mechanical exfoliation method using bulk Kish graphite (Covalent Materials Inc.) *ex situ* in laboratory air (relative humidity ~30–60%) and deposited onto a Si substrate with a 300 nm thick SiO_2 layer. Due to experimental limitations, graphene samples are at least 2–3 days old (initially exposed to laboratory air for a few hours, and then the remaining time in dry nitrogen) before any AFM and adhesion data were acquired. The Si substrate was cleaned before graphene exfoliation using a piranha solution and then rinsed with deionized water (18.2 MΩ resistance). The root-mean-square (RMS) roughness of the Si substrate was found to be ~0.3 nm measured over a 1 × 1 μm^2 area. Graphene samples were then characterized using optical microscopy and Raman spectroscopy to locate areas of interest before conducting AFM measurements. Before adhesion measurements were performed, these areas were again located with the AFM in topographic images acquired in contact/friction mode. The height difference between subsequent layers was then used to confirm the number of layers present in the region of interest. Samples of FLG on muscovite mica (see Supporting Information) were made by mechanical exfoliation onto a freshly-cleaved mica surface inside a sealed chamber purged by clean dry nitrogen (relative humidity <2%).

The bulk graphite sample used in this study is highly ordered pyrolytic graphite (HOPG, SPI Supplies Inc.). All graphite samples were cleaved also *ex situ* in laboratory air and then introduced into the nitrogen-purged AFM chamber with a few minutes, thus minimizing air exposure. Adhesion measurements on freshly-cleaved samples were then conducted within 1 hour of cleaving the sample, while maintaining the low humidity environment. The graphite samples were then "aged" by leaving the samples inside the AFM chamber at <2% RH for a period of 6 days. Under these conditions, the gas environment will have trace amounts of water, oxygen, and other residual species.[26] In both freshly-cleaved and aged graphite samples, regions of interest are those areas having flat terraces greater than 100 nm in lateral dimensions.

We performed single asperity adhesion measurements on these samples in two different series of experiments: (1) direct pull-off measurements; and (2) pre-sliding pull-off measurements. Both measurements utilize force-distance (FD) spectroscopy. In direct pull-off measurements, adhesion measurements were performed using the following protocol. First, once an area of interest was selected, the tip was then slid repeatedly over an area of 20 × 20 nm^2 of a graphene sheet to reduce possible particle contaminants between the tip and surface. Second, after breaking the contact at least once, either 20 or 100 pull-off measurements were acquired at nominally the same area on a region of the graphene sheet at a rate of 1 Hz. Third, the procedure was then repeated at other randomly-selected regions of this area of interest pertaining to graphene having different layer thicknesses. Choosing layer-thicknesses at random allows us to exclude the effect of tip changes on any trends observed as a function of layer thickness. Measured pull-off forces were then averaged for each region, where the error quoted in the pull-off value represents the standard deviation.

In pre-sliding pull-off measurements, the following protocol was followed. First, just as for the case of direct pull-off measurement, once the area of interest was found, the tip was scanned over an area of ~20 × 20 nm^2 to remove tip contamination. Second, the AFM slow-scan direction was disabled to ensure the tip would slide over the same 20 nm line, within the limits of sample/tip drift. Drift was estimated to be 1–2 nm per 30 min of scanning. Third, after 512 cycles of scanning back and forth along the same line at 30 nm/s (total sliding time ~300 s, total sliding distance ~20 μm), scanning was halted and a series of pull-off measurements were then immediately recorded. The pull-off measurement was started from contact with retraction occurring first, so that the pull-off force could be recorded for the first moment the tip broke contact with the surface, and then was approached to the surface to make contact again. Subsequently, 19 additional pull-off measurements were recorded in the same position, *i.e.*, without any lateral motion at a rate of 1 Hz.

FEM Simulations: Additionally, to gain mechanistic information and to mimic the processes governing single asperity adhesion on graphene, finite element method (FEM) simulations were conducted for the case of pre-sliding pull-off measurements. For simplicity, we have simulated a 2-D contact mechanics problem considering adhesive interaction as described in the model in Ref. [17]. Briefly, the model consists of a single layer graphene sheet represented by a thin elastic plate, and the substrate is a rigid body representing the SiO_2 substrate. The tip-graphene interaction is implemented by an effective adhesive force and a frictional shear stress. The values of graphene bending stiffness and in-plane rigidity for graphene were taken from Ref. [33]. Both the tip-graphene interaction strength, w_{tip-gr}, and the graphene-substrate interaction strength, w_{gr-sub}, are described by an effective adhesive potential derived for graphene based on the Lennard-Jones potential by integrating over the surface of the contacting bodies.[34] Using this model, the two types of pull-off measurements described above were simulated. The first case is intended to mimic the direct pull-off measurements, where the tip is brought into contact with the sheet and then immediately withdrawn while the normal force was recorded. In the second case, intended to mimic the pre-sliding pull-off measurements, the same tip was brought into contact with the sheet and then slid along the surface under a compressive normal load until friction reaches a steady-state value. Following sliding, the tip was withdrawn from the surface while the normal force was recorded. We examined the configurations as a function of the interaction ratios between w_{tip-gr} and w_{gr-sub}. Two ratios were examined: 1.2 and 2.0, representing cases with 'fresh' and 'aged' graphene surfaces, respectively. The maximum tensile normal load during retraction was regarded as the pull-off force. For the chosen ratios, we compared the case of regular pull-off *vs.* pre-sliding pull-off, representing the traditional and pre-sliding pull-off measurement, respectively.

Supporting Information

Supporting information is available from the Wiley Online Library or from the author.

Acknowledgements

This work was supported by the National Science Foundation (NSF) under awards NSF/MRSEC (no. DMR-1120901) & NSF/ENG (CMMI-1068741). Q.L. acknowledges support from the National Natural Science Foundation of China (11272177), the 973 Program 2013CB933003 and the Thousand Young Talents Program. P.E. acknowledges financial support from the Natural Sciences and Engineering Research Council (NSERC) of Canada. The authors are grateful for insightful discussions with Dr. P.C. Nalam.

Received: October 7, 2013
Revised: November 19, 2013
Published online: January 22, 2014

[1] K. S. Novoselov, A. K. Geim, S. V. Morozov, D. Jiang, Y. Zhang, S. V. Dubonos, I. V. Grigorieva, A. A. Firsov *Science* **2004**, *306*, 666–669.
[2] S. Bae, H. Kim, Y. Lee, X. Xu, J. S. Park, Y. Zheng, J. Balakrishnan, T. Lei, H. R. Kim, Y. I. Song, *Nat. Nanotechnol.* **2010**, *5*, 574–578.
[3] Y.-M. Lin, C. Dimitrakopoulos, K. A. Jenkins, D. B. Farmer, H.-Y. Chiu, A. Grill, P. Avouris, *Science* **2010**, *327*, 662.
[4] S. P. Koenig, L. Wang, J. Pellegrino, J. S. Bunch, *Nat. Nanotechnol.* **2012**, *7*, 728–732.
[5] D.-E. Jiang, V. R. Cooper, S. Dai, *Nano Letters* **2009**, *9*, 4019–4024.
[6] Y. Han, Z. Xu, C. Gao, *Adv. Funct. Mater.* **2013***23*, 3693–3700.
[7] J. S. Bunch, S. S. Verbridge, J. S. Alden, A. M. van der Zande, J. M. Parpia, H. G. Craighead, P. L. McEuen, *Nano Letters* **2008**, *8*, 2458–2462.
[8] J. Bunch, A. van der Zande, S. Verbridge, I. Frank, D. Tanenbaum, J. Parpia, H. Craighead, P. McEuen, *Science* **2007**, *315*, 490–493.
[9] A. H. Castro Neto, N. M. R. Peres, K. S. Novoselov, A. K. Geim, *Rev. Mod. Phys.* **2009**, *81*, 109–162.
[10] K. S. Novoselov, S. V. Morozov, T. M. G. Mohinddin, L. A. Ponomarenko, D. C. Elias, R. Yang, I. I. Barbolina, P. Blake, T. J. Booth, D. Jiang, J. Giesbers, E. W. Hill, A. K. Geim, *Phys. Status Solidi B* **2007**, *244*, 4106–4111.
[11] S. Chen, Q. Wu, C. Mishra, J. Kang, H. Zhang, K. Cho, W. Cai, A. A. Balandin, R. S. Ruoff, *Nat. Mater.* **2012**, *11*, 203–207.
[12] Y. J. Shin, R. Stromberg, R. Nay, H. Huang, A. T. S. Wee, H. Yang, C. S. Bhatia, *Carbon* **2011**, *49*, 4070–4073.
[13] K.-S. Kim, H.-J. Lee, C. Lee, S.-K. Lee, H. Jang, J.-H. Ahn, J.-H. Kim, H.-J. Lee, *ACS Nano* **2011**, *5*, 5107–5114.
[14] C. Lee, X. Wei, J. Kysar, J. Hone, *Science* **2008**, *321*, 385–388.
[15] G. H. Lee, R. C. Cooper, S. J. An, S. Lee, A. van derZande, N. Petrone, A. G. Hammerberg, C. Lee, B. Crawford, W. Oliver, J. W. Kysar, J. Hone, *Science* **2013**, *340*, 1073–1076.
[16] T. Filleter, J. L. McChesney, A. Bostwick, E. Rotenberg, K. V. Emtsev, T. Seyller, K. Horn, R. Bennewitz, *Phys. Rev. Lett.* **2009**, *102*, 086102.
[17] C. Lee, Q. Li, W. Kalb, X. Liu, H. Berger, R. Carpick, J. Hone, *Science* **2010**, *328*, 76-80.
[18] Z. Deng, A. Smolyanitsky, Q. Li, X. Q. Feng, R. J. Cannara, *Nat. Mater.* **2012**, *11*, 1032–1037.
[19] M. Ishigami, J. Chen, W. Cullen, M. Fuhrer, E. Williams, *Nano Lett* **2007**, *7*, 1643–1648.
[20] Z. Zong, C. Chen, M. Dokmeci, K. Wang, *J. Appl. Phys.* **2010**, *107*, 026104.
[21] S. P. Koenig, N. G. Boddeti, M. L. Dunn, J. S. Bunch, *Nat. Nanotechnol.* **2011**, *6*, 543–546.
[22] Z. Deng, N. N. Klimov, S. D. Solares, T. Li, H. Xu, R. J. Cannara, *Langmuir* **2013**, *29*, 235–243.
[23] W. Gao, R. Huang, *J. Phys. D: Appl. Phys.* **2011**, *44*, 452001.
[24] C. Lui, L. Liu, K. Mak, G. Flynn, T. Heinz, *Nature* **2009**, *462*, 339–341.
[25] R. W. Carpick, M. Salmeron, *Chem. Rev.* **1997**, *97*, 1163–1194.
[26] P. Egberts, Z. Ye, X. Z. Liu, Y. Dong, A. Martini, R. W. Carpick, *Phys. Rev. B* **2013**, *88*, 035409.
[27] K. L. Johnson, *Contact Mechanics*, Cambridge University Press, **1987**.
[28] K. Johnson, K. Kendall, A. Roberts, *Proc. R. Soc. A* **1971**, *324*, 301–313.
[29] B. Derjaguin, V. Muller, Y. P. Toporov, *J. Colloid Interface Sci.* **1975**, *53*, 314–326.
[30] R. J. Cannara, M. J. Brukman, R. W. Carpick, *Rev. Sci. Instrum.* **2005**, *76*, 053706.
[31] Z. Ye, C. Tang, Y. Dong, A. Martini, *J. Appl. Phys.* **2012**, *112*, 116102.
[32] J. E. Sader, J. W. M. Chon, P. Mulvaney, *Rev. Sci. Instrum.* **1999**, *70*, 3967–3969.
[33] M. F. Yu, O. Lourie, M. J. Dyer, K. Moloni, T. F. Kelly, R. S. Ruoff, *Science* **2000**, *287*, 637– 640.
[34] L. Y. Jiang, Y. Huang, H. Jiang, G. Ravichandran, H. Gao, K. C. Hwang, B. Liu, *J. Mech. Phys. Solids* **2006**, *54*, 2436–2452.

